

# The Electromagnetic Design of the X/Y line Combined Function Magnets

N. Tsoupas

August 2024

Collider Accelerator Department  
**Brookhaven National Laboratory**

**U.S. Department of Energy**  
USDOE Office of Science (SC), Nuclear Physics (NP)

Notice: This technical note has been authored by employees of Brookhaven Science Associates, LLC under Contract No. DE-SC0012704 with the U.S. Department of Energy. The publisher by accepting the technical note for publication acknowledges that the United States Government retains a non-exclusive, paid-up, irrevocable, world-wide license to publish or reproduce the published form of this technical note, or allow others to do so, for United States Government purposes.

## **DISCLAIMER**

This report was prepared as an account of work sponsored by an agency of the United States Government. Neither the United States Government nor any agency thereof, nor any of their employees, nor any of their contractors, subcontractors, or their employees, makes any warranty, express or implied, or assumes any legal liability or responsibility for the accuracy, completeness, or any third party's use or the results of such use of any information, apparatus, product, or process disclosed, or represents that its use would not infringe privately owned rights. Reference herein to any specific commercial product, process, or service by trade name, trademark, manufacturer, or otherwise, does not necessarily constitute or imply its endorsement, recommendation, or favoring by the United States Government or any agency thereof or its contractors or subcontractors. The views and opinions of authors expressed herein do not necessarily state or reflect those of the United States Government or any agency thereof.

# The Electromagnetic Design of the X/Y line Combined Function Magnets\*

N. Tsoupas<sup>†</sup>, S. Notaro, J. Best, D. Bruno, D. Holmes, R. Lambiase, G. Mahler, and P-D. Malendele

*Brookhaven National Laboratory, Collider-Accelerator Department, Upton, LI, NY 11973, USA*

---

## Abstract

This technical note presents the electromagnetic design of the combined function magnets which make up the FODO array of the X-line or Y-line magnets of the AGS to RHIC (AtR) transfer line Ref. [1].

Prior to the presentation of the electromagnetic design of the combined function magnets a brief section will be devoted to familiarize the reader with the use of the combined function magnets which make up the elements of the X and Y lines of the AtR line.

*Keywords:* Combined function magnet

---

## 1. Introduction

This technical note presents the Electromagnetic design of the combined function magnets which makes up the FODO arrays of the X-line or Y-line magnets of the AtR line Ref. [1]. A short description of the beam optics of the AtR line will be given, followed by the results of the OPERA computer code Ref. [2] which is used to solve for the electromagnetic properties of the focusing and defocusing combined functions magnets of the X or Y lines which are part of the AtR line.

The results from the solution of the Electromagnetic study of the focusing and defocusing combined function magnets consists of:

---

\*Work supported by the US Department of Energy

<sup>†</sup>tsoupas@bnl.gov

1. The presentation of the B-fields, of the focusing and defocusing combined function magnets, derived from the electromagnetic solution of the magnet models.
2. The coordinates of the reference ray trajectories as the rays transverse the focusing and defocusing magnets.
3. The calculation of the multipoles along the reference trajectory of each magnet.
4. A brief discussion on the survey of the magnets to help the surveyors to position the focusing and defocusing combined function magnets along the beam line.

## **2. A brief description of the AtR beam transfer line.**

The function of the AtR beam transfer line is to transport the beam from the extraction point of the AGS to injection point of the Blue or Yellow rings of the RHIC accelerator for further acceleration and collision of the injected beams Ref. [1].

The beam parameters and the dispersion function along the AtR line are shown in Fig. 1 which shows that the AtR beam transfer line is separated in four sections which are shown in Fig. 1, and briefly described below.

1. The U-line section which transfers the beam from the exit of the AGS to the entrance of the W-line.
2. The W-line section which transfers the beam from exit of the U-line to the entrance of the X or Y line, and also lowers the level of the transferred beam from the AGS level to the level of the RHIC accelerator.
3. The X-line section which injects the beam into the RHIC-Blue ring and the Y-section which injects the beam into the Yellow ring and
4. the M-line which is the injection section of the AtR line which matches the beam parameters of the AtR line into the Blue or Yellow RHIC's injection points.

The separation of the AtR line in the sections, shown in Fig. 1 and mentioned above, is a very convenient way to design the beam optics of the AtR line because the beam parameters of the transfer beam from the exit of the AGS to the injection points of RHIC may change when the ion species transferred along the AtR line also change.

There is a possibility to use the combined function magnets of the X-line, in the new EIC complex to transfer the beam from the end of the AtR line to

the beam injection point of the EIC, because the Y-line magnets will still be used for the beam transfer from the AGS to EIC during the EIC operations. These X-line combined function magnets, being available, will be part of the beam line which will transport the AtR beam from the exit of the Y-line to the injection point at IP4 Ref [3].

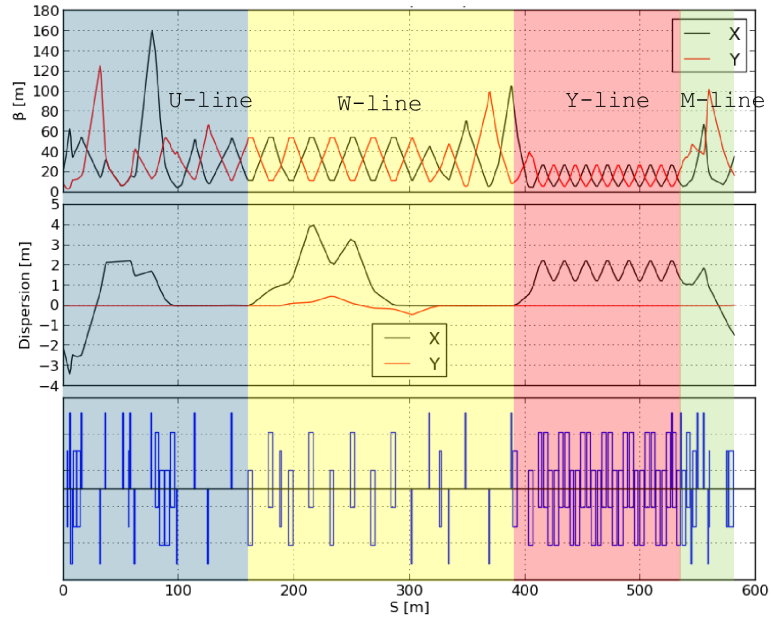


Figure 1: The beam parameters and dispersion functions along the AtR beam transfer line. The "Y-line" section of the AtR line is comprised by the combined function magnets whose electromagnetic properties are discussed in this note.

### 3. The geometry of the X or Y line combined function magnets.

This section provides isometric views of the geometry of the combined function magnets.

An isometric view of the combined function magnet appears in Fig. 2. The green oval shaped object in Fig. 2 is the magnet's vacuum pipe which is made of inconel material.

The red coloured objects are the magnet's coils made of copper material.

The blue and purple coloured objects are the magnetic-iron of the magnet (See Fig. 3 below for the cross section of the iron). The endplates shown in Fig. 4 define the shape of the iron piece at entrance and exit of the magnet (see Fig. 4).

The endplates are machined properly to minimize the 12-pole components of the B-field at the entrance and exit of the magnets.

Although the combined function magnet is a DC magnet, the iron core of the magnets is made up of thin laminations [16 gauge (0.0598") extra low carbon steel] to ease the construction of the magnet.

The cross section of the focusing and defocusing magnets appears in Fig. 3.

29Apr2024 13:45:00

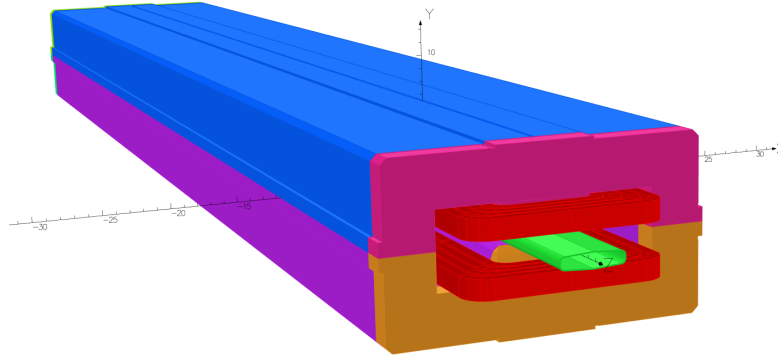


Figure 2: An isometric view of the combined function magnet. The vacuum pipe (green), The coils (red), the top and bottom yoke (blue and purple) see Fig. 3, and the endplates see Fig. 4.

If the beam direction is into the paper, one figure is the focusing and the other the defocusing magnet.

Thus to convert the magnet from focusing to defocusing, the magnet has to be rotated by  $180^\circ$  about the vertical (Y-axis).

It is very important during the survey of the magnets to pay attention to the transverse position of the focusing and defocusing magnets. As shown below there is some difference, in the transverse position of the reference orbit inside the magnet, between the focusing and defocusing magnets.

It is also very important that for both, the focusing and defocusing magnets, the angle of entrance of the reference trajectory, should be equal to the angle of exit. For this to be accomplished, the transverse position of the particle, with the correct rigidity, at the entrance of the magnet must, be very spe-

cific.

It is easy to show, by raytracing a ray with the correct rigidity in the focusing and defocusing magnets, that the transverse position of the ray at the entrance of the magnet is different between the focusing and defocusing magnets.

The different transverse positions for the focusing and defocusing magnets which are shown in Fig. 8 under the label X-Focus, and X-DeFocus, are calculated, and appears in Table 1, and will be used by the surveyors to place the focusing and defocusing magnets along the line.

The isometric view of the endplates is shown in Fig. 4.

The endplates are shown in reddish and brown in Fig. 2, and are chamfered (see Fig. 4) in order to reduce the 12-pole component of the field, at the entrance and exit of the magnet, which would be present if the ends of the pole pieces were not chamfered.

#### **4. The Mechanical Design of the Combined function magnet**

Figure 2 is an isometric view of the combined function magnet. This figure was created by the OPERA computer code after reading the "igs" file of the 3D mechanical design of the magnet.

Figure 3 is the cross section of the magnet for the focusing and defocusing combined function magnets.

Figure 4 the endplates of the magnet. These pieces are made of solid low carbon steel material as the main body of the magnet but one can notice the chamfering of the pole faces, which reduces the 12-pole component of the magnetic field at the entrance and exit of the magnet.

In the OPERA-code the properties of the materials of the magnet and the current density of the coils are assigned. Since the solution of the OPERA model is magnetostatic the only property assigned to the input data is the magnetization curve (BH curve) which appears in Fig. 5.

In this particular case the combined function magnet model was solved by the magnetostatic module of the OPERA code and only the magnetization curve (B,H) was provided.

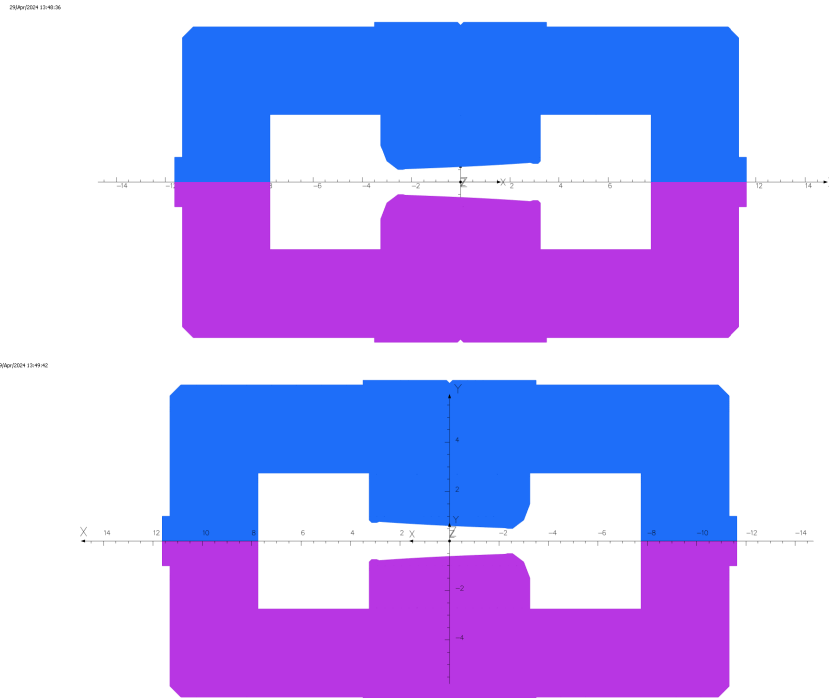


Figure 3: The cross section of the combined function magnet. If the beam direction is into the paper, one orientation is focusing the other defocusing.

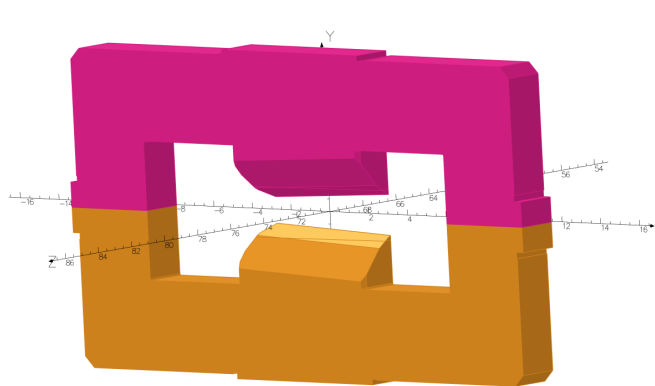


Figure 4: The entrance/exit of the pole pieces of the combine function magnet. Note the chamfering of the pole pieces at the entrance/exit of the magnet.



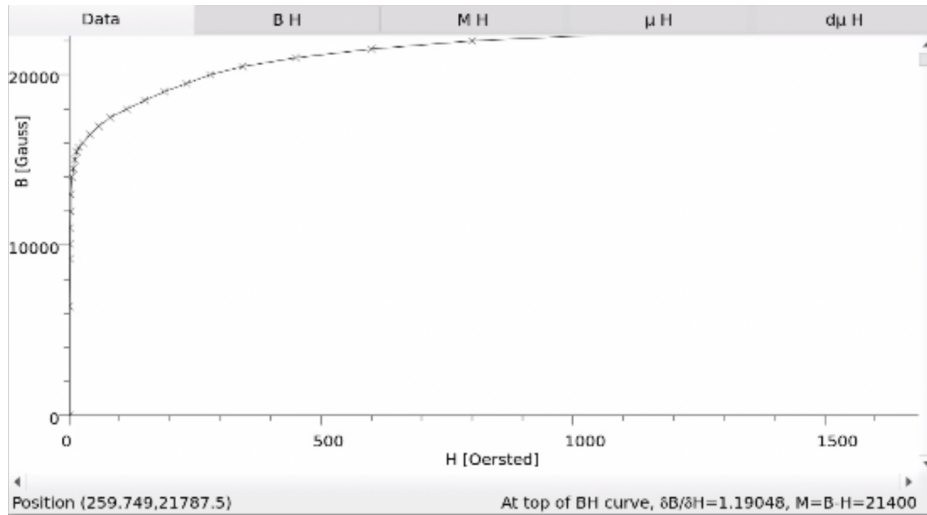


Figure 5: The permeability curve (BH-curve) assigned for the magnetic material of the combined function magnet.

## 5. The Electromagnetic Properties of the Combined function magnet

The igs file of the combined function magnet was read by the OPERA computer code, the property of the magnet's materials (B,H curve) was assigned, and finally the magnet model was meshed and solved under the magnetostatic module of the OPERA code.

A focusing magnet becomes defocusing by rotating the magnets by  $180^\circ$  about the vertical axis (Y-axis) and the solution of both the focusing and defocusing magnets was obtained.

What follows are the plots of magnetic fields as calculated by the OPERA computer code. The  $B_y$  field along the center line of the magnet (Z-direction) appear in Fig. 6 for both, the focusing (black curve) and the defocusing magnet (red curve).

The  $B_y$  fields along the transverse direction (X-axis) at the longitudinal center (Z=0) of the magnet are shown in Fig. 7 for the focusing (black curve) and defocusing (red curve) magnets. Finally the trajectories for the reference orbits should be calculated for the focusing and defocusing magnet.

To obtain these trajectories for a given setting (B-field) of the focusing and defocusing magnet the following conditions should be satisfied by the reference orbits:

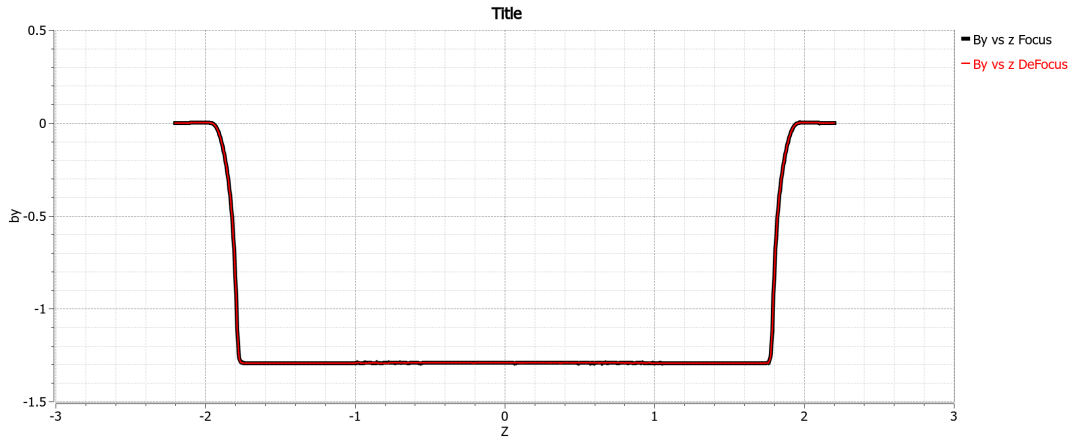


Figure 6: The  $B_y$  field along the center line of the magnet for the focusing and defocusing magnets.

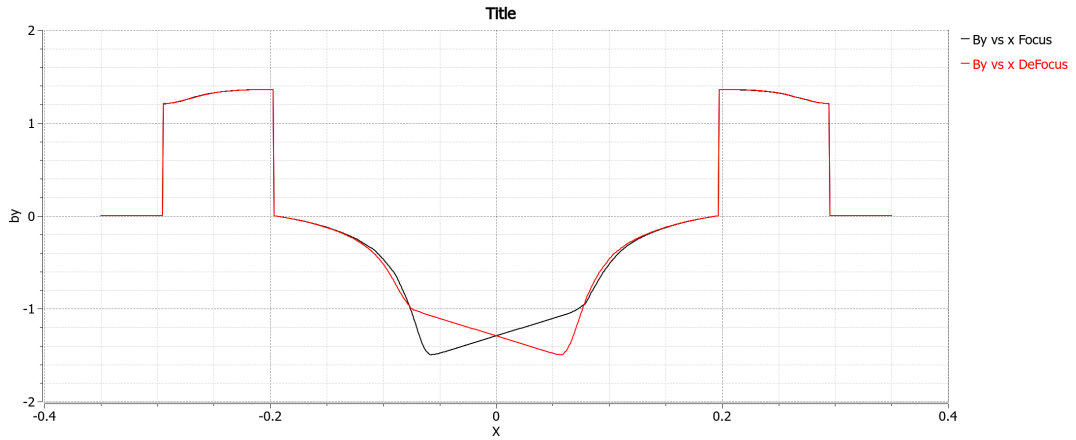


Figure 7: The  $B_y$  field along the transverse direction for the focusing and defocusing magnets.

1. The entrance angle of the reference orbit should be the same as the exit angle, and each angle, should be half of the bending angle.
2. For the above condition to be satisfied the momentum of reference orbit should be the correct momentum and
3. the transverse location of the reference trajectory at the entrance of the magnet, should be the correct one, (see Table 1 ).

The above conditions were satisfied by raytracing rays, using the solutions of

Table 1: Entrance location of reference orbit		
Magnet-Type	X-Focus [mm]	X-DeFocus [mm]
Focusing or Defocus	15	12

the model by the OPERA code and the distances "X-Focus" and "X-Defocus" shown in Fig. 8 were calculated for both the focusing and defocusing magnets.

If the one of the conditions 2 and 3 mentioned above is not satisfied then the condition 1 is not satisfied and trajectory of the reference orbit will be wrong.

The results of this study appear in Fig. 8, which plots the reference trajectories in the focusing and defocusing combined function magnets. These trajectories shown in Fig. 8 show that the trajectory of the reference ray inside the focusing combined function magnet is different from that of the defocusing magnet.

This difference of the central trajectories in the focusing and defocusing

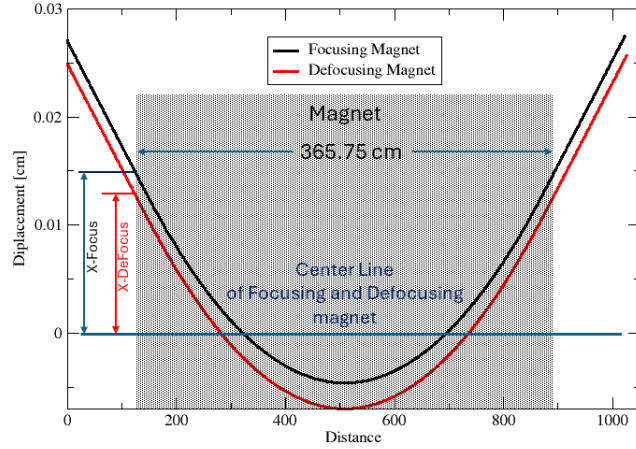


Figure 8: The reference orbits for the focusing and defocusing magnet.

magnets is very important in the survey of the magnet.

This means that the transverse location of the reference ray in the focusing magnet is different from the transverse position in the defocusing magnet. Therefore we should take care when positioning the focusing and defocusing magnets in the transverse direction to ensure the correct transverse locations of the central ray for both, the focusing and defocusing magnets.

Table 1 shows the location of the reference trajectory for the focusing and defocusing magnet in reference to the center line of the magnets.

To complete the calculations of the optical properties of the focusing and defocusing combined function magnets we calculate the magnetic field harmonics (Dipole, quadrupole, sextupole, etc.) for the focusing and defocusing magnets along the reference trajectories of each of the magnets.

These calculations are done as follows:

1. The trajectory  $(x,0,z)$  of the reference particle inside the focusing or defocusing magnets has been calculated to satisfy the conditions mentioned in the previous section.
2. At points along the trajectory of the central orbit (points are separated by 1 cm) in the focusing or defocusing magnet, the magnetic harmonics are calculated on the perimeter of a circle of radius 1 cm. The circle is normal to the trajectory
3. The dipole and quadrupole harmonics are plotted in figures 9 and 10 respectively.
4. From these figures the effective Dipole length, and the effective quadrupole length are calculated.

Figure 9 plots the magnetic field along the reference trajectory of the focusing and defocusing magnets. The iron edges are at  $\pm 1.829$  m from the center of the magnet.

Figure 10 plots the Quadrupole field along the reference trajectory of the focusing and defocusing magnets. The iron edges are at  $\pm 1.829$  m from the center of the magnet. The integral of the Dipole and quadrupole fields along the focusing and defocusing combined function magnets appear in Table 2. It is easy to calculate an effective length for the quadrupole of the focusing and defocusing magnets because the quadrupole field is constant within the magnet as shown in Fig. 10.

This effective length is the ratio of the "Integral-of-Quad-Field"/"Quad-Field-at-Magnet-Center" $=0.1345/0.03744$  m $=3.5924$  m.

To calculate the effective length of dipole field, it is rather difficult because

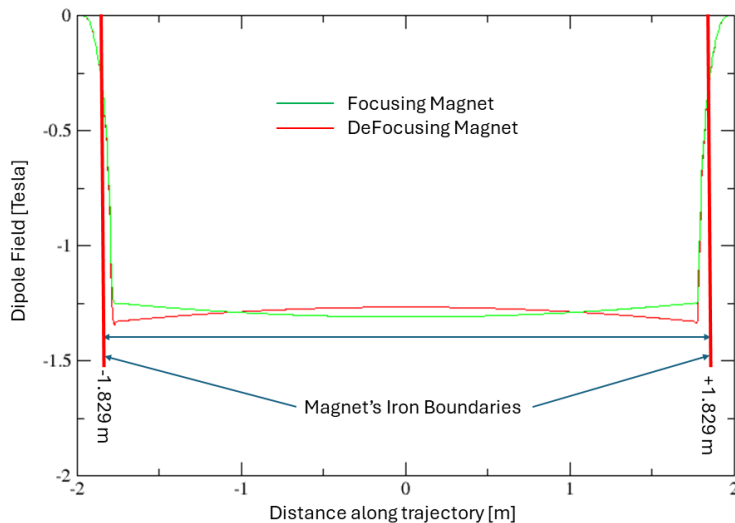


Figure 9: The B-field along the reference trajectory of the focusing and defocusing combined function magnets.

Table 2: Integral of Dipole and Quad fields for Focusing and Defocusing CF magnets

Magnet-Type	Integral Dipole [Tm]	Integral Quad [T]
Focusing	-4.69520	0.134932
Defocusing	-4.69503	-0.135323

the dipole field inside the magnet is not constant along the trajectory of the particle as shown in Fig. 9.

The higher order multipoles starting from Sextupole are very small as shown in Fig. 11 which plots the sextupole multipole along the reference orbit. This indicates that the combined function magnets have been designed very well to generate dipole and quadrupole fields with the higher order multipoles almost negligible.

## 6. Electrical Connection of the Combined Function Magnets

There is a number of 30 identical Combined Function Magnets (CFM) in the X-line which is part of the AtR beam transfer line whose function, currently, is to inject the beam from the AGS extraction point into the Blue

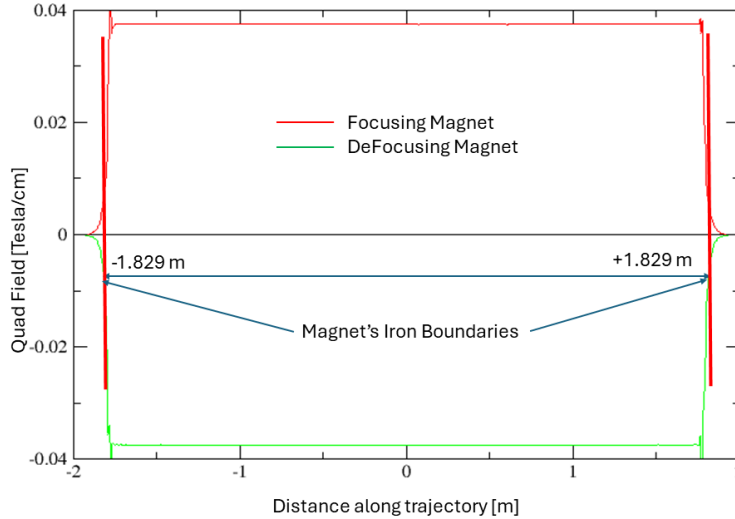


Figure 10: The Quadrupole-field in [T/cm] along the reference trajectory of the focusing and defocusing combined function magnets.

ring of the Relativistic Heavy Ion Collider (RHIC).

With the eRHIC operations, these X-line magnets will be available, therefore, can be use as part of the beam transfer line which will connect the exit of the Y-line to the beam injection point of the Hadron Storage Ring (HSR). In the previous sections of this note the electromagnetic properties of these CFM magnets are described.

In the rest of this section the electrical connection of the 30 CFM magnets will be discussed.

Currently the electrical connection of the X-line combined function magnets follows the sequence FF DD FF DD.....and it appers in Fig. 12.

The new electrical connection will be similar to the one of the X-line magnets shown in Fig. 12 which is described by Ted Robinson Ref. [4].

The main difference of the new electrical connection to the one shown in Fig. 12 is that the new line will be comprised of one of the following sequence of the CFM shown in Table 3.

These 30 CFM will be connected in series and powered by one main power supply. The coils of the combined function magnets are comprised of two circuits, one of  $5 \frac{1}{2}$  turns and a second of  $\frac{1}{2}$  turn creating a total of 4 taps

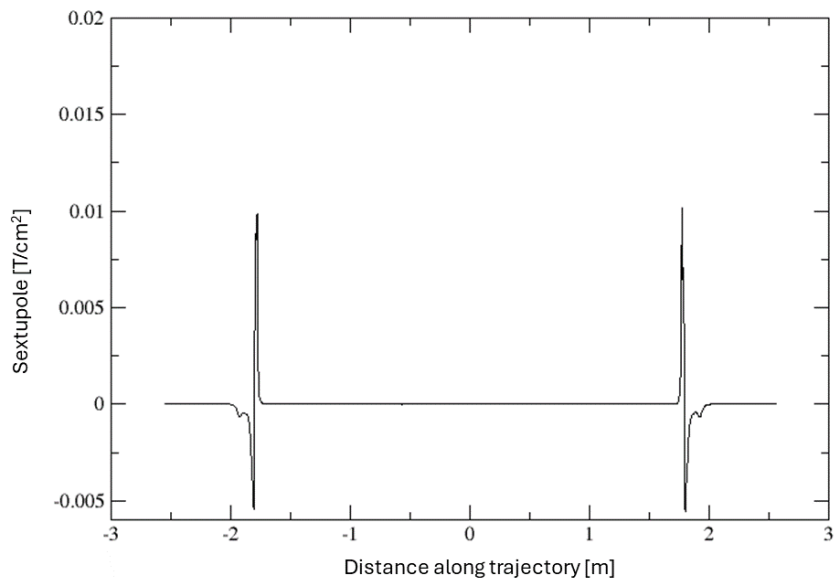


Figure 11: The Sextupole-field in  $[T/cm^2]$  along the reference trajectory of the focusing combined function magnets.

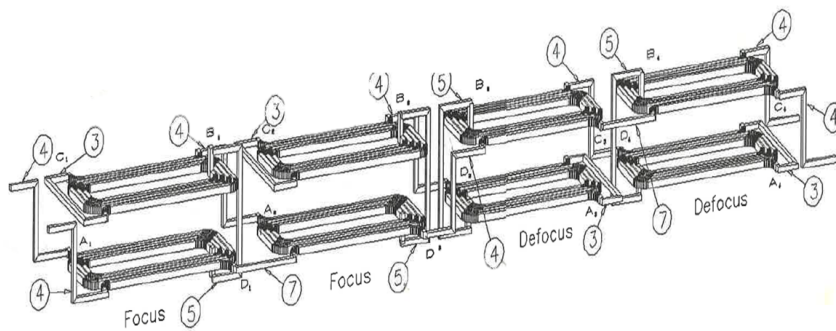


Figure 12: Diagram for connecting the coils of the CFM of the X-line.

Table 3: Two possible ways of connecting the CFM of the new line.

Conection	Magnet Arrangement
1	F D F D
2	F FD F

per coil as shown in Fig. 13.

In this figure, taps for the  $5\frac{1}{2}$  turn circuit are labeled A and B on the top coil while taps for the  $\frac{1}{2}$  turn circuit are labeled C and D.

To avoid having a long return path from the end of the string to the main power supply, the windings of the  $\frac{1}{2}$  turn circuit of the coil is used as part of the return path of the circuit.

Therefore, the  $\frac{1}{2}$  turn circuit must be wired such that the current travels in the same direction as the  $5\frac{1}{2}$  turn circuit. For example, if current travels from tap B to tap A in the  $5\frac{1}{2}$  turn circuit, it must also travel from tap C to tap D in the  $\frac{1}{2}$  turn circuit so that the resulting magnetic field is increased. Configuring the coils like this has the benefit of minimizing the load on the power supply which does not contribute to the magnet's B field, as well as reducing the total space required in the tunnel for cables or water-cooled bus.

There are many possible configurations of bus connections to connect each respective focusing or defocusing magnet to one another.

The chosen configuration of connecting the magnets of the X,Y-line shown in Fig. 12 uses two different bus shapes between magnets, one straight (labeled 7) and the other "Z" shaped (labeled 4). "Z" shaped refers to the bus shape which connects coil taps from the top of one magnet coil to a bottom tap of the next magnet coil, or vice versa.

These inter-magnet connections are made by either a water-cooled copper bus, or a flexible air-cooled braided jumper cable. The buses labeled 3 and 5 Fig. 12 connect coil taps within the same magnet.

With this configuration shown in Fig. 12, the focus-to-focus and defocus-to-defocus magnet pairs can be connected using only 4 unique bus shapes. These bus connections were confirmed by inspecting the combined function magnets installed in the X line.

For the new proposed line which will connect the exit of the Y-line to the injection point of the HSR there are two possible ways, mentioned earlier, to connect the X-line combine function magnets.

The bus connection of the F D F D type of electrical conection of the coils of the CFM appears in Fig. 14.



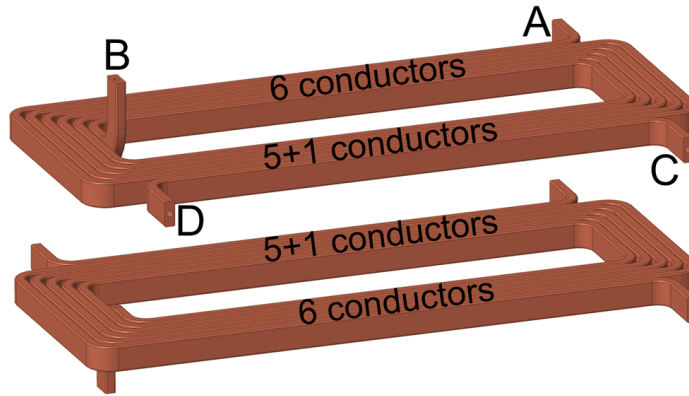


Figure 13: The top and bottom coils of the defocusing CFM. Notice that the top coil of the defocusing magnets consists of 6-conductors and 5+1 conductors on the opposite side. Similarly, the bottom coil consists of 5+1 conductors and 6 conductors on the other side. The actual coil length-to-width ratio has been modified for clarity..

The bus connection of the F FD F type of electrical connection of the coils of the CFM appears in Fig. 15.

—

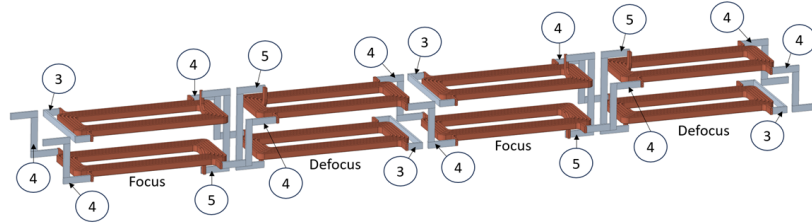


Figure 14: Diagram for connecting the coils of the CFM magnets in the FDFD configuration.

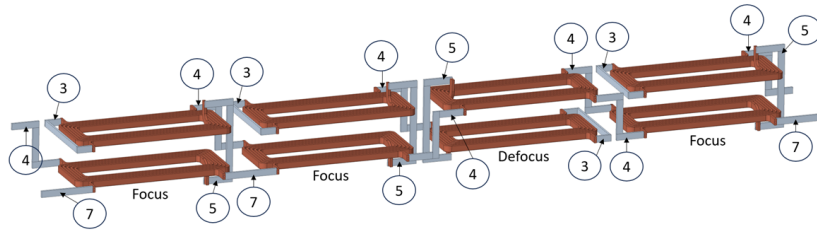


Figure 15: Diagram for connecting the coils of the CFM magnets in the FFDF configuration.

## 7. Conclusions

The Electromagnetic Field calculations of the focusing and defocusing combined function magnets of the AtR X-line have been performed using the OPERA computer code. The results from the calculations show that the

integrated dipole field along the reference beam trajectory for the focusing magnet is practically equal to that of the defocusing magnet. The same also applies for the integrated quadrupole field of the focusing and defocusing magnets except for the sign difference. The design of the magnet is very good for both magnets, focusing and defocusing, to generate extremely small higher order harmonics starting from the sextupole multipole. Great care must be taken in positioning these magnets "transversely" by the surveyors. Finally section 6 discusses the electrical connection of two possible arrangements (Table 1) of connecting the CFM of the new transfer line.

## 8. Acknowledgments

## 9. References

- [1] Focusing and Matching Properties of the AtR Transfer Line  
[https://digital.library.unt.edu/ark:/67531/metadc679353/m2/1/high\\_res\\_d/495791.pdf](https://digital.library.unt.edu/ark:/67531/metadc679353/m2/1/high_res_d/495791.pdf)  
N.Tsoupas et. al.
- [2] <https://www.3ds.com/products/simulia/opera>
- [3] Nick Tsoupas BNL private communication.
- [4] T. Robinson, Coil Configuration, of the CFM January 29, 1992